*32nd EPS Conference on Plasma Phys. Tarragona, 27 June - 1 July 2005 ECA Vol.**29C**, P-5.065 (2005)*

Reversed Current Density in Tokamaks: Equilibrium and Stability Issues

A.A.Martynov[1], S.A.Galkin[1], S.Yu.Medvedev[1], L.Villard[2]

[1]*Keldysh Institute, Russian Academy of Sciences, Moscow, Russia*
[2]*CRPP, Association Euratom-Confédération Suisse, EPFL, Lausanne, Switzerland*

The use of unstructured grids and local refinement adaptation algorithms are attractive tools for the flexible modelling of unusual tokamak equilibrium configurations without nested magnetic flux surfaces. For the numerical solution of Grad-Shafranov equation on triangular grids a special choice of monitor function (error indicator) for adaptation can target several goals: minimization of a solution error, resolution of fast change in the current density profiles, grid packing at chosen magnetic surfaces.

In the frame of classical 1D model exact results are obtained for external kink mode stability of a cylindrical plasma with "current hole" profiles. A key parameter here is a position of zero poloidal field surface. For numerical stability study of the configurations without nested magnetic surfaces the ideas of hybrid finite elements and grid edge alignment to the magnetic surfaces for a good approximation of the MHD spectrum are discussed.

1 Unconventional tokamak equilibria on unstructured adaptive grids

For the numerical solution of Grad-Shafranov equation

$$-R^2\nabla\cdot\left(\frac{\nabla\psi}{R^2}\right)=R^2p'+ff' \tag{1}$$

a standard node-centered finite element code was developed with piece-wise linear basis functions for the solution and piece-wise constant (in cells) approximation of the coefficients and the right hand side.

The grid adaptation technology is based on a combination of isotropic refinement of "macrocells" (triangles or quadrangles) and edge refinement which allows to generate anisotropic grids (triangular cells stretched in the direction of slow change of solution) of acceptable quality [1].

The typical scheme of the problem solution on adaptive grids is as follows:

- An extremely coarse initial grid is uniformly refined several times thus giving the first grid for equilibrium calculation;
- to get the solution on a given grid several Picard iterations are performed;
- a grid adaptation run produces a finer grid according to the chosen "error indicator" and the specified refinement rate (usually 20 per cent). This stage includes also node removal and consistent refinement of the curved boundary.

In all presented examples 8 solution/adaptation cycles were performed that increase the total number of the grid nodes by 5-8 times.

The following error indicator E on the grid edge $\mathbf{e}_{ij}$ was chosen as a value to be equidistributed in the process of local refinement:

$$E=w_1|(\mathbf{e}_{ij}\nabla M)|^p+w_2|(\mathbf{e}_{ij}H(M)\mathbf{e}_{ij}^T)|^p,\quad p=0.5, \tag{2}$$

based on the gradient ∇M and Hessian $H(M)$ of some monitor function M that is chosen to be the following weighted sum: $M=\psi+w_{rhs}M_{rhs}+w_{sep}M_{sep}$. Here the first term is the main part of the indicator related to linear interpolation error of the solution, $M_{rhs}=R^2p'+ff'$ allows to resolve fast change (or discontinuity) of the current density, $M_{sep}=exp(-(\psi-\psi_s)^2/d\psi^2)$ gives the option to pack the grid (in anisotropic manner) to the specified magnetic surface $\psi=\psi_s$ (separatrix in most of the presented examples). The weights are chosen to make the terms dimensionless and reasonably balanced. A justification and an optimization of such choice are open questions.

Two families of force-free configurations were chosen: reversed current equilibria with piece-wise constant ff' [2] and configurations with linear profiles $f(\psi)=\lambda\psi$ reproducing analytical examples from [3].

All the configurations from [2] were recalculated on unstructured grids without special tuning of the error indicator parameters. In analogy with the previous calculations on structured grids solution weighting and feedback shift of the delimiting surface (boundary of reversed current density region) were needed to make the Picard iterations converging.

As one could expect the resolution of the delimiting surface (i.e. current density jump) is essential but the separatrix resolution is not so critical for the solution accuracy. The last option can be more important for stability calculations.

Fig.1 shows the final adaptive grid and solution level lines for negative current hole equilibrium of "central" type that reproduces one of the solutions from Fig.2 in [2]. The separatrix resolution term was turned on for this series. An attempt to go beyond the low current limit mentioned in [2] failed, confirming the fact that there are no such solutions with the chosen topology.

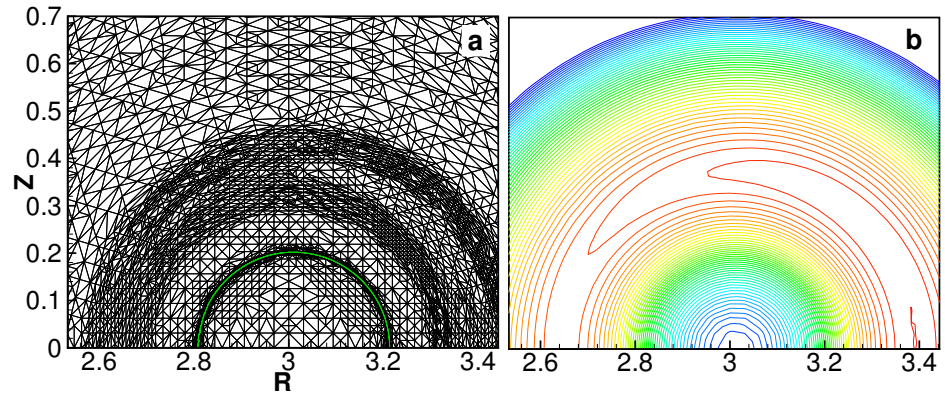

Fig.1. Adaptive grid (a) and solution level lines (b) for reversed current hole case: $I_-/I_+ = -0.1$, $N_{nodes} = 5065$. *The green line shows the delimiting surface.*

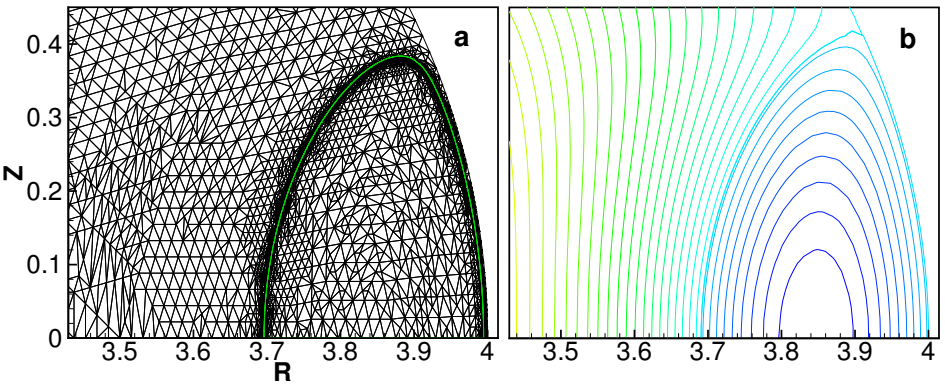

Fig.2. Adaptive grid (a) and level lines for the "dipole" case (b): $I_-/I_+ = -0.28$, $N_{nodes} = 6846$. *The area of negative current density is equal to 0.055 of the total plasma cross-section.*

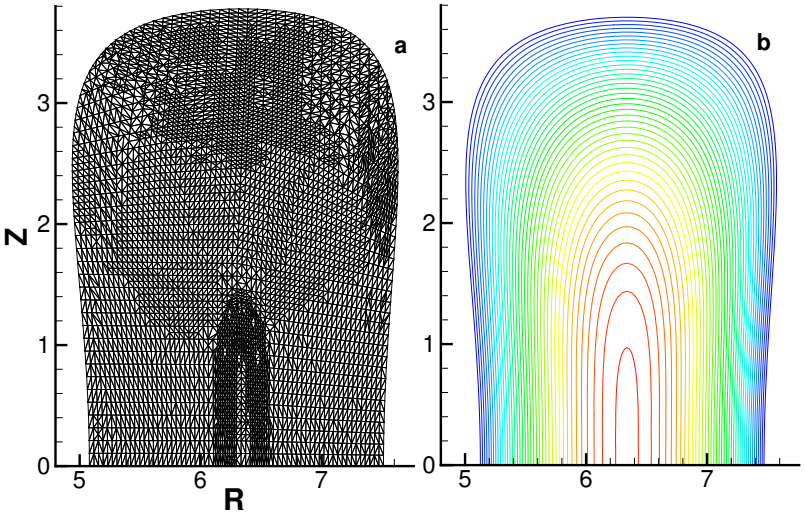

Fig.3. Level lines of the analytic solution (b) with $f = \lambda\psi$, $\psi_{bou} = 0.7$, $\lambda = 0.95$ *and strongly elongated magnetic surfaces near the axis. The grid (a) is specially adapted to the solution value at the magnetic axis,* $N_{nodes} = 8112$.

As for the solutions of "dipole" type, the use of unstructured grids (together with a new option to prescribe the current hole area instead of its diameter) allowed to obtain a solution with smaller negative currents (in absolute value) than in [2] (see Fig.2).

Another family of unconventional equilibria can be generated by indentations in the plasma shape. Analytic force-free configurations with $f = \lambda\psi$ [3] provide a convenient testbed for the new gridding/solution technology. In particular, the configuration with strongly elongated magnetic axis ($\partial^2\psi/\partial z^2 = 0$) looks as a challenge problem for structured grid solvers. Fig.3 shows how this unusual feature is resolved on an unstructured grid with adaptation to the solution maximal value $\psi_s = \psi_{max}$ in the last term of the error indicator (2).

2 External kink mode stability: 1D cylindrical model

A cylindrical plasma with periodic boundary conditions in a strong longitudinal magnetic field ($B_\theta \ll B_z$) is a classical model for study of external kink mode stability [4]. In some simple cases (piece-wise constant current density and $B_z = constant$) it is possible to get analytical results. Here we consider the following model for tokamak "current hole" distribution in terms of normalized minor radius $x = r/a$:

$$j_z = \left\{ \begin{array}{ll} j_- \leqslant 0, & 0 \leqslant x < x_{ds}, \\ 1, & x_{ds} \leqslant x < x_1, \\ 0, & x_1 \leqslant x < 1. \end{array} \right\}. \tag{3}$$

The "hollow current" case, $j_- = 0$, was considered in [5]. Here we revise those results and show how negative core current density influences external kink mode stability.

It is convenient to introduce the parameter $u = x^2$ and ratio of total negative and positive currents, $I_- = u_{ds}j_-/(u_1 - u_{ds}) \leqslant 0$. Then the safety factor profile related to its edge value q_a takes the form:

$$q(u)/q_a = \left\{ \begin{array}{ll} u_{ds}(1 + 1/I_-), & 0 \leqslant u < u_{ds}, \\ u(u_1 - u_0)/(u - u_0), & u_{ds} \leqslant u < u_1, \\ u, & u_1 \leqslant u < 1, \end{array} \right\} \tag{4}$$

with the singular point

$$u_0 = u_{ds}(1 - j_-) = u_{ds} - I_-(u_1 - u_{ds}) \tag{5}$$

which corresponds to the zero poloidal field surface.

The free boundary cylindrical plasma stability (with conducting wall at infinity) in the limit $R/a \sim B_z/B_\theta \to \infty$ is determined by the following potential energy minimum expression (omitting some positive multipliers) [4]

$$W = \xi^2(1)B_\theta^2(1)[(1-t)^2(1+m) - 2(1-t) + (1-t)^2(r\xi'/\xi)|_{x=1}], \tag{6}$$

here $t = nq_a/m$, $\xi(x)$ is the radial component of the corresponding (m, n) harmonic of the displacement vector $\vec{\xi}(r)exp(i(m\theta - nz/R))$ satisfying the following Euler equation:

$$[x^3(1/q - n/m)^2\xi']' = x(1/q - n/m)^2(m^2 - 1)\xi. \tag{7}$$

Specifics of the "current hole" profiles (3),(4) is the presence of an internal resonant surface, $q(u_s) = m/n$, at the point $u_s = x_s^2 = u_0/(1-t(u_1-u_0))$. In this case the function $\xi(x)$ minimizing the potential energy functional is zero inside the surface $0 \leqslant x \leqslant x_s$ [4] and can be analytically calculated outside taking into account the condition of normal perturbed magnetic field continuity at x_s: $(krB_z + mB_\theta(x_s))\xi(x_s + 0) = 0$.

Finally, the following inequalities give necessary and sufficient conditions for kink mode instability

$$\frac{F(\mu)}{u_1} < t < 1, \quad F(\mu) = \left[1 - \frac{1-\mu^m}{m(1-\mu)}\right]\left[1 - \mu\frac{1-\mu^m}{m(1-\mu)}\right]^{-1} \tag{8}$$

with $\mu = u_s/u_1 = (u_0/u_1)/(1 - tu_1(1 - u_0/u_1))$.

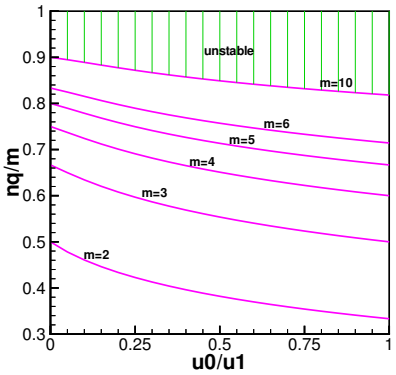

Fig.4. Stability diagram.

The left inequality in (8) can be resolved giving the critical value of the parameter $tu_1 = nq_{min}/m$ versus the value of u_0/u_1 and poloidal wave number m. The result is presented at the stability diagram, Fig.4. For a given value of u_0/u_1 the harmonic (m, n) is unstable if $nq_a/m < 1$ and nq_{min}/m exceeds the corresponding critical value.

The diagram allows us to make some conclusions on external kink mode stability of "current hole" configurations compared to a standard monotonic profile:

- The left boundary of the diagram, $u_0/u_1 = 0$, reproduces the classical result of [4] for monotonic current density profile: the critical value for nq_{min}/m is $(m-1)/m$. In particular, a global shear value $q_a/q_{min} > 2$ (i.e. $u_1 < 1/2$) guarantees stability for all the modes $m > 1$ and all the values of $q_a > 1$.
- "Current hole" profiles ($u_0 > 0$) make the stability properties worse: higher values of global shear are needed for stability. In the worst case of delta-function profile, $u_0/u_1 \to 1$, the critical value for nq_{min}/m is $(m-1)/(m+1)$. In particular, a global shear value $q_a/q_{min} > 3$ (i.e. $u_1 < 1/3$) provides stability for all the modes.
- Compared to "hollow" current density ($I_- = 0$), the appearance of negative core current has some destabilizing effect due to the outside shift of zero poloidal field surface u_0 according to the formula (5). Thus the unstable region in q-values broadens.
- The same results on stability are valid for arbitrary current density profile in the region $0 \leqslant u \leqslant u_{ds}$ provided that the integral current is non-positive there, $I_- \leqslant 0$.

3 Stability: Discussion on numerical methods

For the stability study of configurations without nested magnetic surfaces the most general and promising approach would be to give up the use of special coordinates and magnetic surface projections.

Some experience in treating a similar kind of problem, namely the equation in the limit of ideal plasma, retaining all the unknown electric field projections, showed that the use of numerical approximation similar to hybrid finite elements is sufficient for a quite accurate representation of the ideal MHD spectrum for force-free plasmas [6] without using magnetic projections.

The development of a new ideal MHD stability code on unstructured 2D grids can employ an approach close to the primal hybrid finite elements [7] in order to adequately represent the degrees of freedom of the original differential problem. Another issue is the role of grid edge alignment to the magnetic surfaces for a good approximation of MHD spectrum.

Acknowledgements The CRPP author is supported in part by the Swiss National Science Foundation.

References

[1] A.A. Martynov, S.Yu. Medvedev, in Grid generation: theory and applications, Moscow 2002 (in Russian), http://www.ccas.ru/gridgen/ggta02/abstracts.html
[2] A.A.Martynov, S.Yu.Medvedev, L.Villard, Phys. Rev. Lett. **91**(2003)85004
[3] A.A. Martynov, S.Yu. Medvedev, Plasma Phys. Reports, 28, 259-267 (2002)
[4] V.D.Shafranov, JTF, 40, 241-252 (1970)
[5] L.M. Degtyarev, A.G. Kirov, A.A. Martynov *et al.*, KIAM Preprint N28 (1983)
[6] S.A.Galkin, A.A.Ivanov, S.Yu.Medvedev *et al.*, Comp. Phys. Comm. 143, 29-47 (2002)
[7] P.A.Raviart, J.M.Thomas, Math. of Comp., 31, 391-413 (1977)